MATH 174 Project: 4D Helix

Oras Phongpanangam

Abstract

I studied the 4-dimensional counterpart to the 3-dimensional curves, and applied the methodology specifically to 4D helix, the special curve where the curvature and torsion are constants. In 3D, these constraints result in a circular helix, spiraling into infinity. However, in 4D, it turns out the properties of a curve with constant curvature, torsion, and "bitorsion", the new quantity arising in the fourth dimension, are much different to the 3D counterpart. In fact, it might have more in common with the 2D circle, and I hypothesize that the patterns continue on in an alternating sequence at higher and higher dimensions.

I worked out the generalization of the Frenet-Serret formulas, or just Frenet formulas for short, to the four-dimensional $\mathbb{R}^4$. Using the formulas, I was able to calculate the position of a curve as parametrized by arclength. I then studied the 4D helix using several projections and visualization techniques, revealing its properties.

1 Generalized Frenet Apparatus

I find dimensional analogy to be one of the most useful tools in investigating higher dimensions. Imagine a plane curve in our three-dimensional space. We see that we have one vector, the binormal, staying constant and normal to the plane the curve is embedded in. Once we deconfine the curve from the plane, the binormal vector comes alive, and varies along with the tangent and the normal vector.

In the four dimensional case, I suspect that there will be four principle vectors forming an orthonormal frame in $\mathbb{R}^4$. When we have a curve embedded in a three-dimensional subspace, the fourth vector should be held consant, and normal to the entire subspace. The torsion quantity characterizes how the curve fails to lie in a plane, so perhaps there will be a new quatity that characterizes how a curve fails to fit in a hyperplane.

In trying to generalize the Frenet apparatus to the fourth dimension, the first challenge I faced was the binormal vector, B. In the three dimensional case, we define it as $B = T \times N$. However, cross products are only defined in $\mathbb{R}^3$, so this definition will not generalize to $\mathbb{R}^4$.

By inspecting the Frenet formulas:

$$\begin{aligned} T' &= \quad\quad \kappa N \quad\quad\quad\quad \\ N' &= -\kappa T \quad\quad\quad +\tau B \\ B' &= \quad\quad -\tau N \quad\quad\quad\quad \end{aligned}$$

I decide to try defining B by using the second row:

$$N' = -\kappa T + \tau B$$
$$\Rightarrow B = \frac{1}{\tau} N' + \frac{\kappa}{\tau} T.$$

assuming $\tau \neq 0$. We just need B to be a unit vector, so redefine the quantity τ as

$$\tau = |N' + \kappa T|$$

Now, we can redefine B as

$$B = \frac{1}{\tau}(N' + \kappa T)$$

This way, B is defined only in terms of T and N using differentiation and dot products, all of

which are generalizable to $\mathbb{R}^4$. This definition will also preserve the third row formula:

$$\begin{aligned}(B\cdot T)' &= B'\cdot T + T'\cdot B\\ &= B'\cdot T + \kappa N\cdot(\frac{1}{\tau}N' + \frac{\kappa}{\tau}T)\\ &= B'\cdot T + 0 = 0\end{aligned}$$

$$\Rightarrow B'\cdot T = 0$$

$$\begin{aligned}(B\cdot N)' &= B'\cdot N + N'\cdot B\\ &= B'\cdot N + (\frac{1}{\tau}N' + \frac{\kappa}{\tau}T)\cdot N'\\ &= B'\cdot N + \frac{1}{\tau}|N'|^2 + \frac{\kappa}{\tau}T\cdot N'\\ &= B'\cdot N + \frac{1}{\tau}(\kappa^2+\tau^2) - \frac{\kappa^2}{\tau}\\ &= B'\cdot N + \tau = 0\end{aligned}$$

$$\Rightarrow B'\cdot N = -\tau$$

$$(B\cdot B)' = 2B'\cdot B = 0$$

$$\Rightarrow B'\cdot B = 0$$

We can then define the fourth vector of the orthonormal basis as the unit vector normal to T, N, and B at once. For now, I choose to call this vector Q for "Quad", or something that has to do with number four. So we have

$$\begin{aligned}Q\cdot T &= 0\\ Q\cdot N &= 0\\ Q\cdot B &= 0\\ Q\cdot Q &= 1\end{aligned}$$

We can now then investigate Q', the fourth row of the Frenet formulas.

1.1 The Fourth Row

Using the usual trick of differentiating a dot product can take us far. First, note that for any orthogonal, unit vectors A and B, we have

$$\begin{aligned}A\cdot B &= 0\\ (A\cdot B)' = A'\cdot B + A\cdot B' &= 0\\ A'\cdot B &= -A\cdot B'\end{aligned}$$

and also

$$\begin{aligned}A\cdot A &= 1\\ (A\cdot A)' = 2A'\cdot A &= 0\\ A'\cdot A &= 0\end{aligned}$$

These generalize the manipulation of vector B above to any pair of any vectors from the apparatus. This means that in the Frenet formula table of any dimensionality, the antisymmetric structure will be preserved always. We now know that

$$Q'\cdot Q = 0.$$

By definition, $T' = \kappa N$, so $T'\cdot Q = 0$. By antisymmetry, we also have

$$Q'\cdot T = 0$$

Now, consider $Q\cdot B$:

$$\begin{aligned}Q\cdot B &= 0\\ &= Q\cdot\left(\frac{1}{\tau}N' + \frac{\kappa}{\tau}T\right)\\ &= \frac{1}{\tau}Q\cdot N'\\ \Rightarrow Q\cdot N' &= 0\end{aligned}$$

By antisymmetry,

$$Q'\cdot N = 0$$

Therefore, Q' is only pointing in the B direction. Define

$$Q' = -\xi B$$

because I like the letter ξ, and the sign gives us a nice pattern. As per professor Farris's suggestion, I decided to call ξ the "bitorsion" of the

curve. We now have enough information to fill in the Frenet formulas table for $\mathbb{R}^4$:

$$\begin{array}{llll} T' = & & \kappa N & \\ N' = & -\kappa T & & +\tau B \\ B' = & & -\tau N & & +\xi Q \\ Q' = & & & -\xi B \end{array}$$

1.2 Notes on the direction of Q

In 3D, if we define the binormal vector B as the unit vector normal to both T and N, there are two possible vectors that fit the description, pointing the opposite direction to each other. To keep the definition consistent, we define B based on the right hand rule of cross product, namely, that $B = T \times N$. This way, the formulas work out as intended.

In 4D, we don't have the luxury of the cross product, and so the orientation of vectors become more difficult to discern. The right hand rule won't make much sense in 4D, unless we have some kind of an alian hand to work with. With our definition of Q above, we face the same problem in defining the direction of Q as in the 3D case. In this project, I choose to solve this problem by defining ξ to be a positive quantity. This way, I define Q to be the component of the vector B' not in the direction of N, namely

$$Q = \frac{1}{\xi}(B' + \tau N)$$

where I define $\xi = |B' + \tau N|$, which I decide to call. With this formulation, we don't have the theory of a signed bitorsion, but that will not be necessary for my analysis as done in this paper. If one would like to use a signed bitorsion, it is possible to define Q based on the orientation of T, N, and B using a higher analogy of the cross product, but I will not explore it in this paper.

1.3 Properties of Bitorsion ξ

For space curves, τ can be thought of as a measure for how much the curve fails to fit on a plane. As it turns out, ξ can be thought of as an analogy to that, telling us how much a curve fails to be a space curve. If ξ is identically zero, and $\tau > 0$ and $\kappa > 0$, then the curve must be a space curve.

The proof is similar to the 3D case. Assume that for a unit speed curve α, $\kappa > 0, \tau > 0, \xi = 0$. Then, $Q' = 0$, thus Q is a constant vector. Examine $(\alpha(s) - \alpha(0)) \cdot Q$. We have

$$\begin{aligned} [(\alpha(s) - \alpha(0)) \cdot Q]' &= \alpha'(s) \cdot Q \\ &= T \cdot Q \\ &= 0 \end{aligned}$$

Thus, $(\alpha(s) - \alpha(0)) \cdot Q$ is a constant. We can find its value by examining the case when $s = 0$, where clearly $((\alpha(s) - \alpha(0)) \cdot Q = 0 \cdot Q = 0$. Therefore, $\alpha(s) - \alpha(0)$ is always perpendicular to Q. This means that Q is perpendicular to the 3D subspace α lives in, and thus α is a space curve.

Note that this is only true when $\kappa > 0$ and $\tau > 0$ at all positions. We have seen some examples of space curves with $\tau = 0$ that fail to be a plane curve because there are points where κ vanishes. This should analogously be true for 4D curves as well.

2 Plotting the 4D Helix

With the Frenet formulas derived, it is possible to solve the differential equations to obtain the positions α at any given arclength. I was particularly interested in the special curve where $\kappa = \tau = \xi = 1$. It is of course possible to derive the curve with κ, τ, and ξ as any function of arclength s. The initial conditions I used were

$$\begin{aligned} \alpha(0) &= (0, 0, 0, 0) \\ T(0) &= (1, 0, 0, 0) \\ N(0) &= (0, 1, 0, 0) \\ B(0) &= (0, 0, 1, 0) \\ Q(0) &= (0, 0, 0, 1) \end{aligned}$$

Using SageMath's numerical integration module with the differential equations from the generalized Frenet formulas, the approximation for α

is found. I then used orthogonal projection into four directions, x, y, z, and w, to visualize the curve in 3D. I also tried stereographic projection, but the results were largely the same so I did not include them here. Figure 2.1 shows the four projections of the curve.

The most distinctive feature of the curve has to be the fact that it closes around itself into a torus-like structure in all directions. This means that unlike the 3D case, where the helix goes off to infinity, constant curvature, torsion, and bitorsion is enough to confine the 4D curve in a bounded space. This is analogous to the 2D case, where a constant curvature yields a circle, which also loops into itself. My question was: what is the shape that the curve is confined to? My project aims to answer that question, and I successfully did so.

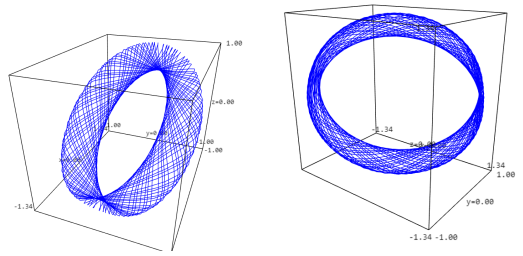

(a) xyz (b) xyw

(c) xzw (d) yzw

Figure 2.1: Four orthogonal projections of α using coordinates selection

2.1 Involute Curve

Using the usual formula

$$E(s) = \alpha(s) - sT$$

the involute curve can be generalized easily to 4D. An orthogonal projection is shown in Figure 2.2. In 3D, the evolute of a helix would be a plane curve. Sadly, this is not true in 4D. Using the Frenet formulas, ξ of the evolute is found to fluctuate between 0.02 and 7, far from being identically 0. It doesn't seem like the evolute is particularly revealing of the curve. Though it is worth noting that numerical derivative is sensitive to the error of the values, especially for an oscillatory function like α we have, so this may not be accurate.

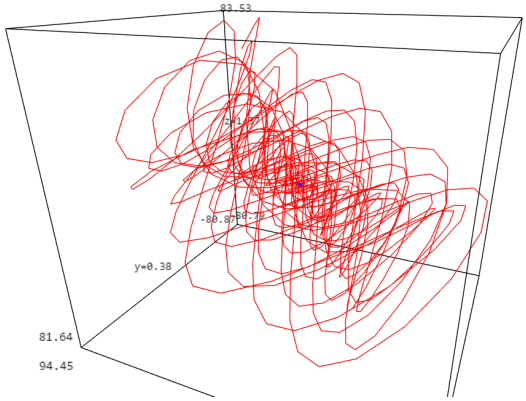

Figure 2.2: The xyz orthogonal projection of the involute curve

2.2 Evolute Curve

Similarly, the formula

$$I(s) = \alpha(s) + \frac{1}{\kappa}N(s)$$

allows us to generalize the evolute curve to 4D. The four orthogonal projections are shown in Figure 2.3. Similarly to the involute, the value of ξ is found to fluctuate between 1.68 and 5.36, and is not particularly revealing.

As it turned out, for this project, I found many numerical methods used in data science to be extremely helpful in visualizing this 4D object, even more so than the traditional geometrical techniques. The same remark about error above applies here.

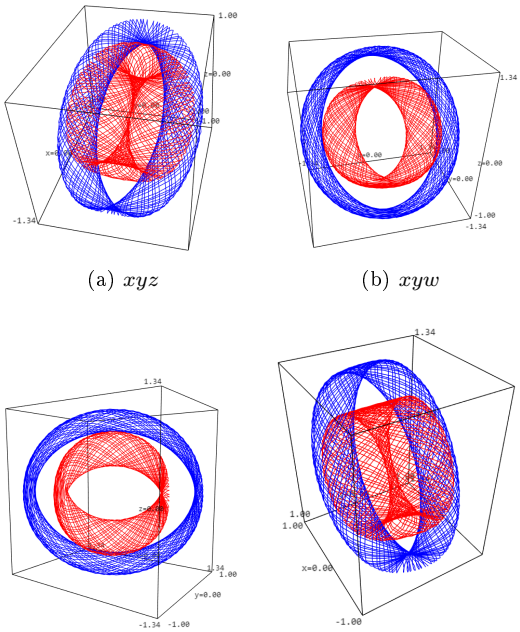

(a) xyz (b) xyw

(c) xzw (d) yzw

Figure 2.3: Four orthogonal projections of the evolute curve (red) inside α (blue)

3 Numerical Analyses

Using SageMath, which is based on Python, I instinctively reached for many traditional techniques used in data science, most of which are very readily available as Python libraries. I find these methods very powerful in visualizing highly multidimensional data. While projections can give us a clue to the actual the shape of the object, we inevitably lose the information of a dimension everytime we project the object down to a lower dimension. Graphing, on the other hand, can visualize every dimension and how they interplay with each other at once. While we lose the visual aspect of the object, we are able to comprehend all dimensions at the same time, powerfully complementing the technique of projection.

3.1 α Plots

A very simple thing to do is to plot out the values of α at each position, with one line corresponding to one dimension. As Figure 3.1 shows, the values in all directions are clearly oscilatory in nature, confirming my suspicion that the 4D helix loops back onto itself.

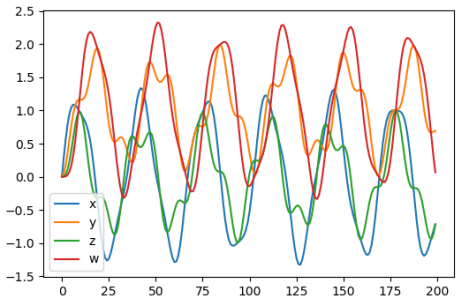

Figure 3.1: Values of each direction of α as varying with s

3.2 Center of Mass Plots

Center of mass of the curve shows where the curve is centered at. The center of mass of a curve as s increases is given as

$$cm = \frac{\int_0^s \alpha(s')ds'}{s}$$

For 3D helix, the center of mass will move toward infinity as the curve itself extends. The plot of center of mass of the 4D helix is shows in Figure 3.2, the values calculated numerically. Clearly, the position of the center of mass approaches a certain point, approximately $(0, 1, 0, 1)$, showing that the curve is indeed bounded, and centered at $(0, 1, 0, 1)$.

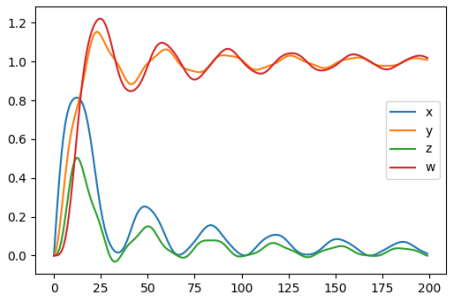

Figure 3.2: The center of mass of α

3.3 Principal Component Analysis (PCA)

Though having its root in statistics, principal component analysis or PCA is a very powerful technique widely used in data science and machine learning, particularly in data visualization. PCA is defined as an orthogonal transformation of a vector space based on a set of points such that the variance of the points as measured along a basis vector is maximized. The result is usally the more "correct" projection of the data, showing more vividly the underlying characteristic of a set of data, and making it possible to discard dimensions with less information.

Let the set of n points in an m-dimensional space be represented by an $n \times m$ matrix X, with each row representing a point. PCA is equivalent to the eigen-decomposition of the covariance matrix of X, namely

$$X^T X = M \Lambda M^T$$

where Λ is the diagonal matrix with eigenvalues in each diagonal cell, and M the eigenmatrix representing the orthogonal transformation, with an eigenvector as each column.

Call the values of α in the PCA basis $\alpha_{pca} = \alpha M$. Figure 3.3 shows the α and α_{pca} space curve of a 3D helix when solved from the differential equation using the initial condition $\alpha(0) = (0,0,0), T(0) = (1,0,0), N(0) = (0,1,0), B(0) = (0,0,1)$. Note that α is moving in the diagonal direction, due to the unsuitable initial conditions, but α_{pca} moves along the x-axis nicely. Figure 3.4 shows the values of 3D α and α_{pca} as a line plot. Notice that in α_{pca}, the x direction increases linearly, showing clearly how the helix is extending in only 1 direction.

Figure 3.5 shows the plot of the 4D helix α_{pca}. Note that the curves look much more sinusoidal than the α plot, hinting at the nicer nature of this basis.

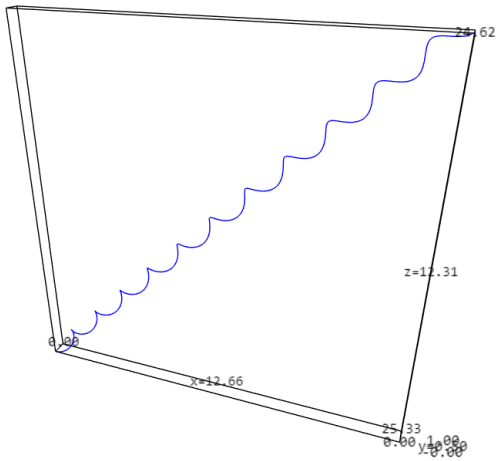

(a) α

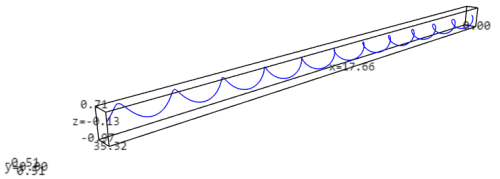

(b) α_{pca}

Figure 3.3: 3D helix before and after PCA treatment

4 Putting Them All Together

Numerical results told us a few things. First, the α plot confirms that the curve is bounded and oscillatory. Second, the center of mass plot

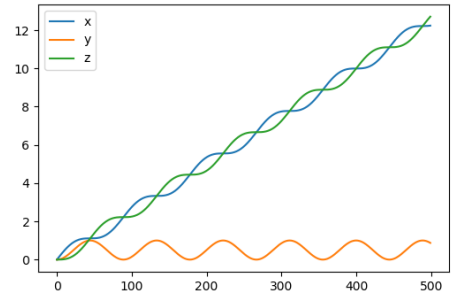

(a) α

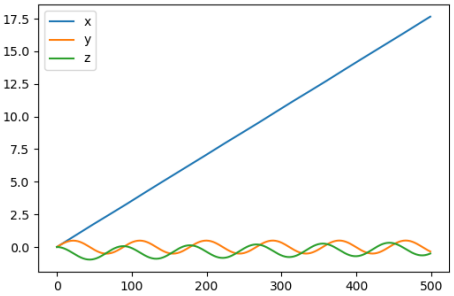

(b) α_{pca}

Figure 3.4: Values of α and α_{pca} of 3D helix

shows that the curve is off-center. To recenter the curve, I changed the initial condition of α to $\alpha(0) = (0, -1, 0, -1)$, simply to offset the center back to zero. With a centered curve, hopefully PCA will perform better as well.

The results were of great satisfaction. Figure 4.1 shows the α values and the center of mass of the centered curve. The curve is centered at much closer to 0 than before, as the range of the oscillations shows. But perhaps the most satisfying was the plot of α_{pca}, shown in Figure 4.2. The graphs become purely sinusoidal, varying at shared 2 magnitudes. In fact, as Figure 4.3 shows, xy and zw form sine and cosine pairs of the same frequency and magnitude, each tracing out a circle. This is where I recognize the

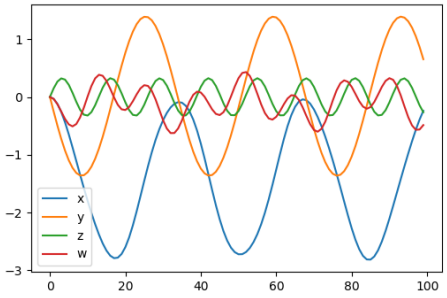

Figure 3.5: Values of α_{pca} of 4D helix

curve as being on a 4D flat torus, given by

$$x(u, v) = (r_1 \cos(u), r_1 \sin(u), r_2 \cos(v), r_2 \sin(v))$$

From the numerical result, this torus has $r_1 = 0.327$ and $r_2 = 1.377$.

Figure 4.4 shows the four orthogonal projections of α_{pca}, and Figure 4.5 shows the four orthogonal projections of the flat torus given by $x(u, v) = (0.327\cos(u), 0.327\sin(u), 1.377\cos(v), 1.377\sin(v))$. Notice that they look exactly the same. Thus it becomes very clear that α indeed lies on a flat torus. It is quite interesting how a 4D curve, with four directions to vary in, is confined to only a 2-manifold in $\mathbb{R}^4$. So while α with such simple κ, τ, and ξ looked chaotic at first, it is in fact greatly uniform.

5 Miscellaneous

5.1 Aside on Higher Dimensions

Considering the generalized 4D Frenet formulas, it becomes quite clear that the formulas can be extended easily to any number of dimensions. Operating on that assumption and continuing the antisymmetric pattern downward, I derived the 5D Frenet formulas and plotted out a 5D helix with all the differential invariants equal to one. The result, shown as α and α_{pca} plots in

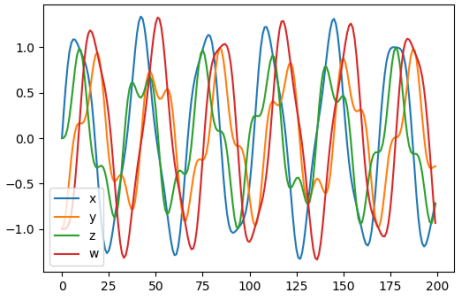

(a) α plot

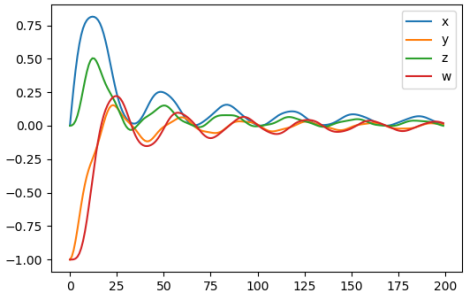

(b) center of mass plot

Figure 4.1: Plots of the centered α

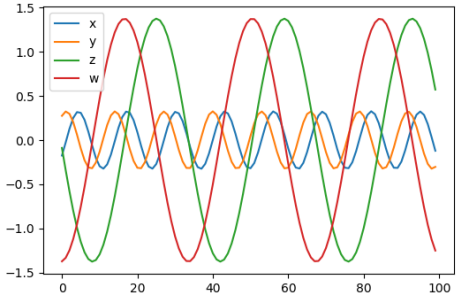

Figure 4.2: α_{pca} of the centered 4D helix

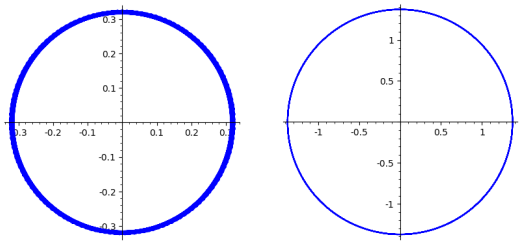

(a) xy (b) zw

Figure 4.3: 2D projections of α

Figure 5.1, shows that the curve once again extends to infinity in one direction, much like the 3D helix. Figure 5.2 shows the 6D version, showing the oscillatory nature again. Remember that the 2D helix, which is a circle, is also oscillatory and bounded. It is then my hypothesis that this pattern continues alternatedly as the number of dimensions increases.

5.2 Acknowledgement of the Lack of Mathematical Rigor

I relied heavily on numerical methods in this project, so this might not seem very satisfactory to a pure mathematician. Particularly, the fact that the 4D helix lies on a flat torus is realized through a series of plots and graphs, not through symbolic manipulation. It is also possible that the numerical results contain hidden errors from the lack of infinite precision, especially when calculating the differential invariants. However, since we are dealing with a smooth, well-behaved curve, the plots of α should be very accurate, and they show without a doubt that the flat torus is the underlying shape of α. It is also worth noting that symbolic computation of the 4D helix was extremely chaotic and did not reveal much about the curve, and was computationally intensive. Rather, the numerical methods used here ran on my tiny laptop without a hiccup, and can be applied to study much more complex curves. It is my belief that though not exactly precise, these techniques have their place in studying geometry.

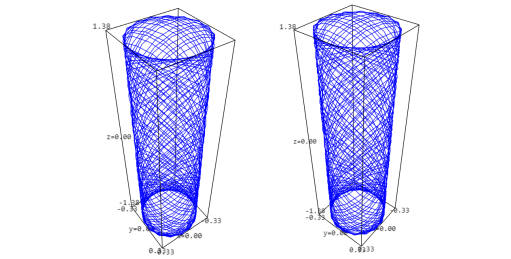

(a) xyz (b) xyw

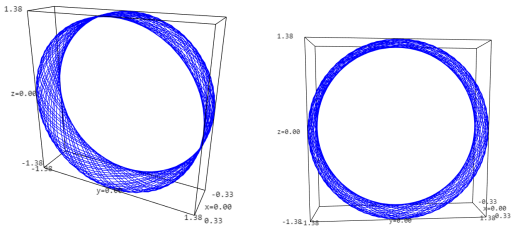

(c) xzw (d) yzw

Figure 4.4: Four orthogonal projections of centered α_{pca}

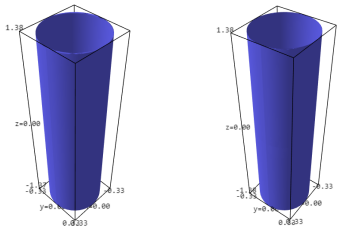

(a) xyz (b) xyw

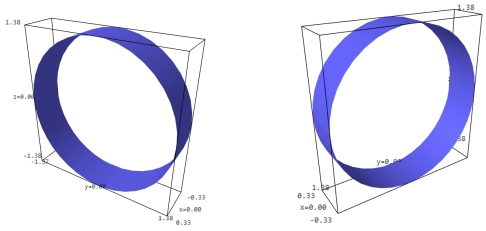

(c) xzw (d) yzw

Figure 4.5: Four orthogonal projections of the flat torus

5.3 Possible Further Works

- Though already shown through plots, it will be much more satisfying if I can work out a proof that 4D helix indeed lies on a flat torus with mathematical rigor.
- This project only studied the curve with $\kappa = \tau = \xi = 1$. There are infinite possibilities these values can have, and there are many other curves to study.
- The values of κ, τ, and ξ should dictate the shape of the flat torus the 4D helix lies on, characterized by the 2 radii. It should be possible to work out how to determine exactly the shape of such a torus.
- Plots shown above gave us a glimpse at the beautiful pattern of alternating behavior between divergence and convergence of the helices at higher dimensions. It will be exciting to prove that this is indeed true, and why so.

6 Conclusion

I find numerical methods and data visualization techniques to be greatly applicable to geometry of higher dimensions. Data science deals with highly multidimensional data all the time, so it is quite possible that there are even more sophisticated techniques that can be applied to higher dimensional geometry. I'd be excited to keep my eyes out for more of them.

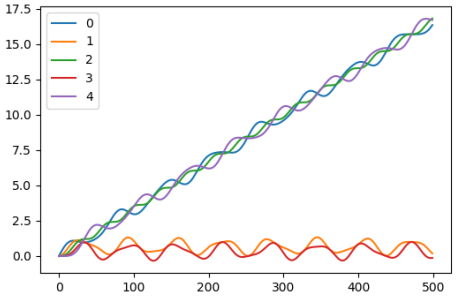

(a) α

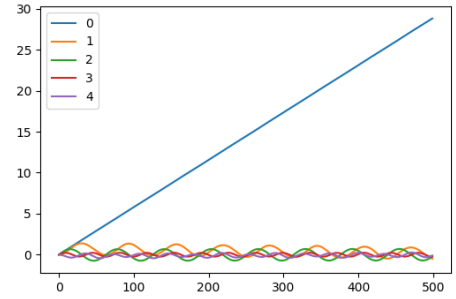

(b) α_{pca}

Figure 5.1: 5D helix before and after PCA treatment

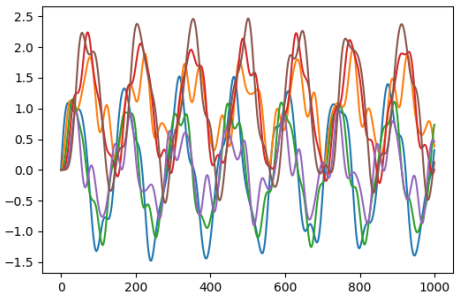

(a) α

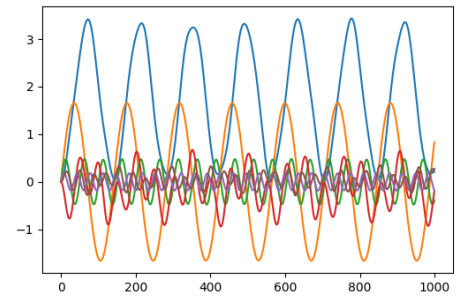

(b) α_{pca}

Figure 5.2: 6D helix before and after PCA treatment